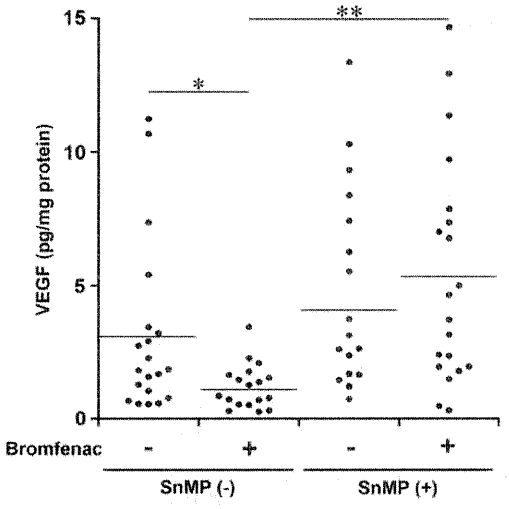

Figure 9 VEGF level of intraocular fluid in each eye was plotted. Analysis of intraocular fluid using ELISA showed that intraocular VEGF level was lower in bromfenac-treated rat ($^{*}P < 0.01$). Additional injection of SnMP increased intraocular VEGF level as high as in control CNV rats ($^{**}P < 0.001$). No significant difference resulted from intraperitoneal SnMP alone. Each group contained 20 samples from 20 eyes ($n = 20$). Mean value of each group was expressed by a line. The corrected significant *P*-value (Mann–Whitney *U*-test) was defined as 0.0125 after Bonferroni correction.

after a long period.[7,10] Topical NSAIDs had therapeutic effects on CNV in this study. Because it has such a potentially neuroprotective effect, combination therapy with an anti-VEGF drug may be very advantageous for patients. Combination therapy is found to be more effective, but is less likely to result in drug resistance than mono-therapy in the t reatment of tumor angiogenesis.[51] In addition, repeated intravitreal injections were necessary for the majority of patients to maintain this level of benefit.[4,5] Intravitreal injections can be physically uncomfortable, and they expose the patient to a number of potential vision-threatening complications such as intraocular infection. Topical administration of a drug that has the capacity to substantially reduce CNV would be a promising advance in the development of therapies for neovascular eye diseases. Finally, there was a technical problem in this study. RT-PCR might be more suitable for objective quantification of invading macrophages. We performed RT-PCR using a primer for macrophage; however, no reproducible data were obtained (data not shown). The results were strongly affected by the size of photocoagulation spot or sampling biases. This limitation should be also noted.

In conclusion, the present study showed a new mechanism of NSAIDs for inhibiting neovascularization of the choroid. Topical NSAIDs would be beneficial for the treatment of CNV not only because of its anti-angiogenic effect but also its potential anti-stress effect. Because the CNV model can be a mirror for other angiogenic diseases in the central nervous system, NSAIDs could be studied more widely and profoundly as a candidate therapy for these disease conditions (Supplementary Figure 1).

Supplementary Information accompanies the paper on the Laboratory Investigation website (http://www.laboratoryinvestigation.org)

ACKNOWLEDGEMENTS

This work was supported by a grant from the Research Committee on Chorioretinal Degeneration and Optic Atrophy, Ministry of Health, Labor, and Welfare, Tokyo, Japan; and by a Grant-in-Aid for Scientific Research from the Ministry of Education, Science, and Culture of the Japanese Government, Tokyo, Japan.

DISCLOSURE/CONFLICT OF INTEREST

The authors declare no conflict of interest.

1. Bressler NM, Bressler SB, Fine SL. Age-related macular degeneration. Surv Ophthalmol 1988;32:375–413.
2. Soubrane G. Choroidal neovascularization in pathologic myopia: recent developments in diagnosis and treatment. Surv Ophthalmol 2008;53:121–138.
3. Cohen SY, Laroche A, Leguen Y, *et al.* Etiology of choroidal neovascularization in young patients. Ophthalmology 1996;103: 1241–1244.
4. TAP study group. Photodynamic therapy of subfoveal choroidal neovascularization in age-related macular degeneration with verteporfin: one-year results of 2 randomized clinical trials–TAP report. Treatment of age-related macular degeneration with photodynamic therapy (TAP) Study Group. Arch Ophthalmol 1999;117:1329–1345.
5. Rosenfeld PJ, Brown DM, Heier JS, *et al.* Ranibizumab for neovascular age-related macular degeneration. N Engl J Med 2006;355:1419–1431.
6. Nishijima K, Ng YS, Zhong L, *et al.* Vascular endothelial growth factor-A is a survival factor for retinal neurons and a critical neuroprotectant during the adaptive response to ischemic injury. Am J Pathol 2007;171:53–67.
7. Robinson GS, Ju M, Shih SC, *et al.* Nonvascular role for VEGF: VEGFR-1, 2 activity is critical for neural retinal development. FASEB J 2001;15:1215–1217.
8. Murakami Y, Ikeda Y, Yonemitsu Y, *et al.* Inhibition of choroidal neovascularization via brief subretinal exposure to a newly developed lentiviral vector pseudotyped with Sendai viral envelope proteins. Hum Gene Ther 2010;21:199–209.
9. Saint-Geniez M, Kurihara T, Sekiyama E, *et al.* An essential role for RPE-derived soluble VEGF in the maintenance of the choriocapillaris. Proc Natl Acad Sci USA 2009;106:18751–18756.
10. Rosenfeld PJ, Shapiro H, Tuomi L, *et al.* Characteristics of patients losing vision after 2 years of monthly dosing in the phase III ranibizumab clinical trials. Ophthalmology 2011;118:523–530.
11. Sakamoto T, Soriana D, Nassaralla J, *et al.* Effect of intravitreal administration of indomethacin on experimental subretinal neovascularization in the subhuman primate. Arch Ophthalmol 1995; 113:222–226.
12. Takahashi H, Yanagi Y, Tamaki Y, *et al.* COX-2-selective inhibitor, etodolac, suppresses choroidal neovascularization in a mice model. Biochem Biophys Res Commun 2004;325:461–466.
13. Takahashi K, Saishin Y, Saishin Y, *et al.* Topical nepafenac inhibits ocular neovascularization. Invest Ophthalmol Vis Sci 2003;44:409–415.
14. Yanni SE, Clark ML, Yang R, *et al.* The effects of nepafenac and amfenac on retinal angiogenesis. Brain Res Bull 2010;81:310–319.
15. Kim SJ, Toma HS. Inhibition of choroidal neovascularization by intravitreal ketorolac. Arch of Ophthalmol 2010;128:596–600.
16. Kim SJ, Toma HS, Barnett JM, Penn JS. Ketorolac inhibits choroidal neovascularization by suppression of retinal VEGF. Exp Eye Res 2010;91:537–543.
17. Wilson HL, Schwartz DM, Bhatt HR, *et al.* Statin and aspirin therapy are associated with decreased rates of choroidal neovascularization among patients with age-related macular degeneration. Am J Ophthalmol 2004;137:615–624.

18. Rezaei KA, Toma H, Cai J, *et al.* Reduced choroidal neovascular membrane formation in cyclooxygenase-2 null mice. Invest Ophthalmol Vis Sci 2010;52:701–707.
19. Tegeder I, Pfeilschifter J, Geisslinger G. Cyclooxygenase-independent actions of cyclooxygenase inhibitors. FASEB J 2001;15:2057–2072.
20. Ponka P. Cell biology of heme. Am J Med Sci 1999;318:241–256.
21. Maines MD. The heme oxygenase system: a regulator of second messenger gases. Annu Rev Pharmacol Toxicol 1997;37:517–554.
22. Brouard S, Otterbein LE, Anrather J, *et al.* Carbon monoxide generated by heme oxygenase 1 suppresses endothelial cell apoptosis. J Exp Med 2000;192:1015–1026.
23. Alcaraz MJ, Habib A, Créminon C, *et al.* Heme oxygenase-1 induction by nitric oxide in RAW 264.7 macrophages is upregulated by a cyclo-oxygenase-2 inhibitor. Biochim Biophys Acta 2001;1526:13–16.
24. Hou CC, Hung SL, Kao SH, *et al.* Celecoxib induces heme-oxygenase expression in glomerular mesangial cells. Ann NY Acad Sci 2005; 1042:235–245.
25. Nascimento-Silva V, Arruda MA, Barja-Fidalgo C, *et al.* Novel lipid mediator aspirin-triggered lipoxin A4 induces heme oxygenase-1 in endothelial cells. Am J Physiol Cell Physiol 2005;289:C557–C563.
26. Grosser N, Abate A, Oberle S, *et al.* Heme oxygenase-1 induction may explain the antioxidant profile of aspirin. Biochem Biophys Res Commun 2003;308:956–960.
27. Cantoni L, Valaperta R, Ponsoda X, *et al.* Induction of hepatic heme oxygenase-1 by diclofenac in rodents: role of oxidative stress and cytochrome P-450 activity. J Hepatol 2003;38:776–783.
28. Arimura N, Ki-i Y, Hashiguchi T, *et al.* Intraocular expression and release of high-mobility group box 1 protein in retinal detachment. Lab Invest 2009;89:278–289.
29. Otsuka H, Arimura N, Sonoda S, *et al.* Stromal cell-derived factor-1 is essential for photoreceptor cell protection in retinal detachment. Am J Pathol 2010;177:2268–2277.
30. Fujimoto T, Sonoda KH. Choroidal neovascularization enhanced by Chlamydia pneumoniae via Toll-like receptor 2 in the retinal pigment epithelium. Invest Ophthalmol Vis Sci 2010;51:4694–4702.
31. Honda M, Sakamoto T, Ishibashi T, *et al.* Experimental subretinal neovascularization is inhibited by adenovirus-mediated soluble VEGF/flt-1 receptor gene transfection: a role of VEGF and possible treatment for SRN in age-related macular degeneration. Gene Ther 2000;7:978–985.
32. Aburaya M, Tanaka K-I, Hoshino T, *et al.* Heme oxygenase-1 protects gastric mucosal cells against non-steroidal anti-inflammatory drugs. J Biol Chem 2006;281:33422–33432.
33. Jones MK, Wang H, Peskar BM, *et al.* Inhibition of angiogenesis by nonsteroidal anti-inflammatory drugs: insight into mechanisms and implications for cancer growth and ulcer healing. Nat Med 1999;5: 1418–1423.
34. Jones MK, Szabó IL, Kawanaka H, *et al.* von Hippel Lindau tumor suppressor and HIF-1alpha: new targets of NSAIDs inhibition of hypoxia-induced angiogenesis. FASEB J 2002;16:264–266.
35. Ferrara N. Vascular endothelial growth factor and the regulation of angiogenesis. Recent Prog Horm Res 2000;55:15–35.
36. Tsutsumi C, Sonoda KH, Egashira K, *et al.* The critical role of ocular-infiltrating macrophages in the development of choroidal neovascularization. J Leukoc Biol 2003;74:25–32.
37. Ghosh S, May MJ, Kopp EB. NF-kappa B and Rel proteins: evolutionarily conserved mediators of immune responses. Annu Rev Immunol 1998;16:225–260.
38. Jaiswal AK. Nrf2 signaling in coordinated activation of activation of antioxidant gene expression. Free Radic Biol Med 2004;36: 1199–1207.
39. Kaspar JW, Niture SK, Jaiswal AK. Nrf2:INrf2 (Keap1) signaling in oxidative stress. Free Radic Biol Med 2009;47:1304–1309.
40. Healy ZR, Lee NH, Gao X, *et al.* Divergent responses of chondrocytes and endothelial cells to shear stress: cross-talk among COX-2, the phase 2 response, and apoptosis. Proc Natl Acad Sci USA 2005;102: 14010–14015.
41. Bussolati B, Ahmed A, Pemberton H, *et al.* Bifunctional role for VEGF-induced heme oxygenase-1 *in vivo*: induction of angiogenesis and inhibition of leukocytic infiltration. Blood 2004;103:761–766.
42. Dulak J, Loboda A, Zagórska A, Józkowicz A. Complex role of heme oxygenase-1 in angiogenesis. Antioxid Redox Signal 2004;6: 858–866.
43. Bussolati B, Mason JC. Dual role of VEGF-induced heme-oxygenase-1 in angiogenesis. Antioxid Redox Signal 2006;8:1153–1163.
44. Mandal MN, Patlolla JM, Zheng L, *et al.* Curcumin protects retinal cells from light-and oxidant stress-induced cell death. Free Radic Biol Med 2009;46:672–679.
45. Shyong MP, Lee FL, Hen WH, *et al.* Viral delivery of heme oxygenase-1 attenuates photoreceptor apoptosis in an experimental model of retinal detachment. Vision Res 2008;48:2394–2402.
46. Sun MH, Su Pang JH, Chen SL, *et al.* Retinal protection from acute glaucoma-induced ischemia-reperfusion injury through pharmacological induction of heme oxygenase-1 by cobalt protoporphyrin. Invest Ophthalmol Vis Sci 2010;51:4798–4808.
47. Qin S, McLaughlin AP, De Vries GW. Protection of RPE cells from oxidative injury by 15-deoxy-delta12,14-prostaglandin J2 by augmenting GSH and activating MAPK. Invest Ophthalmol Vis Sci 2006;47: 5098–5105.
48. Gamache DA, Graff G, Brady MT, *et al.* Nepafenac, a unique non-steroidal prodrug with potential utility in the treatment of trauma-induced ocular inflammation. I: assessment of anti-inflammatory efficacy. Inflammation 2000;24:357–370.
49. Isaka M, Inada K, Tsutsumi S, *et al.* Ocular tissue distribution in rabbit after instillation of bromfenac sodium ophthalmic solution. Drug Metabol Pharmacokinet 1999;14:32–41.
50. Kida T, Ogawa T, McNamara TR, *et al.* Evaluations of the human COX-1 and COX-2 inhibition for amfenac, bromfenac, ciclofenac, and ketorolac. Annu Meet Guide Abstr Am Coll Clin Pharm 2007; (Suppl):274.
51. Abdollahi A, Folkman J. Evading tumor evasion: current concepts and perspectives of anti-angiogenic cancer therapy. Drug Resist Updat 2010;13:16–28.

Published OnlineFirst August 4, 2011; DOI:10.1158/1078-0432.CCR-11-1477

Clinical Cancer Research

microRNA-10b: A New Marker or the Marker of Pancreatic Ductal Adenocarcinoma?

Tetsuro Setoyama, Xinna Zhang, Shoji Natsugoe, et al.

Clin Cancer Res 2011;17:5527-5529. Published OnlineFirst August 4, 2011.

Published OnlineFirst August 4, 2011; DOI:10.1158/1078-0432.CCR-11-1477

Clinical Cancer Research

CCR Translations
Commentary on Preis et al., p. 5812

microRNA-10b: A New Marker or the Marker of Pancreatic Ductal Adenocarcinoma?

Tetsuro Setoyama[1,4], Xinna Zhang[2,3], Shoji Natsugoe[4], and George A. Calin[1,3]

microRNA-10b (miR-10b) expression in pancreatic ductal adenocarcinoma (PDAC), as identified by *in situ* hybridization, is highly correlated with cancer diagnosis, therapy response, and prognosis. If these findings are further confirmed in prospective studies, miR-10b could be used to improve the management of PDAC and decrease the mortality rate of this deadly cancer. *Clin Cancer Res; 17(17); 5527–9.* ©*2011 AACR.*

In this issue of *Clinical Cancer Research*, Preis and colleagues (1) report that the level of microRNA-10b (miR-10b) expression, as found using *in situ* hybridization (ISH) of endoscopic ultrasonography (EUS)–guided fine needle aspiration (FNA) biopsy samples, was significantly correlated with response to neoadjuvant therapy and outcome in pancreatic ductal adenocarcinoma (PDAC).

This study is important for several reasons. First, the authors wisely focused on a deadly type of cancer, PDAC, which is the fourth leading cause of cancer death and the second most common gastrointestinal malignancy in the United States. The median survival duration of PDAC patients is 4.4 months, and the 5-year survival rate is around 4% for all PDAC patients (2). At present, no established biomarkers for early diagnosis and prognosis exist; therefore, it is imperative that we find new predictors for both patients and clinicians. Carcinoembryonic antigen (CEA) and cancer antigen 19-9 (CA19-9) are regarded worldwide as standard adjunctive markers, but their levels are also elevated in benign and other malignant conditions; thus, they are not recommended for diagnosis or prognosis by the American Society of Clinical Oncology (3).

Second, the identified gene, *miR-10b*, makes functional sense as being intimately linked to the mechanism of metastasis, the cause of most PDAC deaths. microRNAs (miRNA) are 19- to 25-nucleotide (nt) noncoding RNAs (ncRNA) and are already classic examples of RNA molecules that do not codify for proteins. By degrading or blocking translation of mRNA targets, these miRNAs can regulate a large part of the mammalian genome, including genes involved in metastases (4). miRNAs are also involved in the initiation and progression of human cancers (5) and can behave as oncogenes or tumor suppressors (4). Among miRNAs, miR-10b was the first that was found, by Ma and colleagues (6), to be correlated with metastasis in breast cancer. It is induced by the epithelial–mesenchymal transition–related transcription factor Twist and suppresses HOXD10, which represses several genes that contribute to cell migration and extracellular matrix remodeling in breast cancer, RhoC, urokinase plasminogen activator receptor, a3-integrin, and MT1–matrix metalloproteinase (MMP; ref. 6). Another target of miR-10b is Kruppel-like factor 4 (KLF4), which acts as a transcriptional factor. In esophageal cancer cells, miR-10b was found to directly suppress KLF4, promoting cancer invasion (7). One target of miR-10b is the tumor suppressor neurofibromin; in neurofibromatosis malignant peripheral nerve sheath tumor cells, miR-10b directly suppresses the mRNA of neurofibromin, and RAS signaling in these cells is activated (8). In contrast, T lymphoma invasion and metastasis 1 (TIAM1) was identified as an additional target gene for miR-10b; silencing TIAM1 caused suppression of breast cancer cell migration (Fig. 1A; ref. 9).

Third, the authors used adequate material for the study. EUS-FNA is highly accurate at identifying patients with suspected PDAC, especially when other modalities have failed, and has rare complications (10). EUS-FNA biopsy specimens are as reliable as surgical tissues, with a reported positive predictive value, negative predictive value, and accuracy rate of 99%, 64%, and 84%, respectively. EUS-FNA biopsy is a sensitive method, but false-negative cases must also be evaluated (10). EUS-FNA biopsy is done before therapy, allowing the clinician to predict response or outcome. Preis and colleagues used a highly sensitive fluorescence-based ISH technique combined with immunohistochemical analysis with cytokeratin 19 to identify epithelial cells in EUS-FNA biopsy specimens. This method was not time consuming and enabled them to evaluate the

Authors' Affiliations: Departments of [1]Experimental Therapeutics and [2]Cancer Biology and [3]Center for RNA Interference and Non-Coding RNAs, The University of Texas MD Anderson Cancer Center, Houston, Texas; [4]Department of Surgical Oncology and Digestive Surgery, Graduate School of Medical and Dental Sciences, Kagoshima University, Kagoshima, Japan

Corresponding Author: George A. Calin, Department of Experimental Therapeutics, Unit 36, The University of Texas MD Anderson Cancer Center, Houston, TX 77030. Phone: 713-792-5461; Fax: 713-745-4528; E-mail: gcalin@mdanderson.org

doi: 10.1158/1078-0432.CCR-11-1477

Published OnlineFirst August 4, 2011; DOI:10.1158/1078-0432.CCR-11-1477

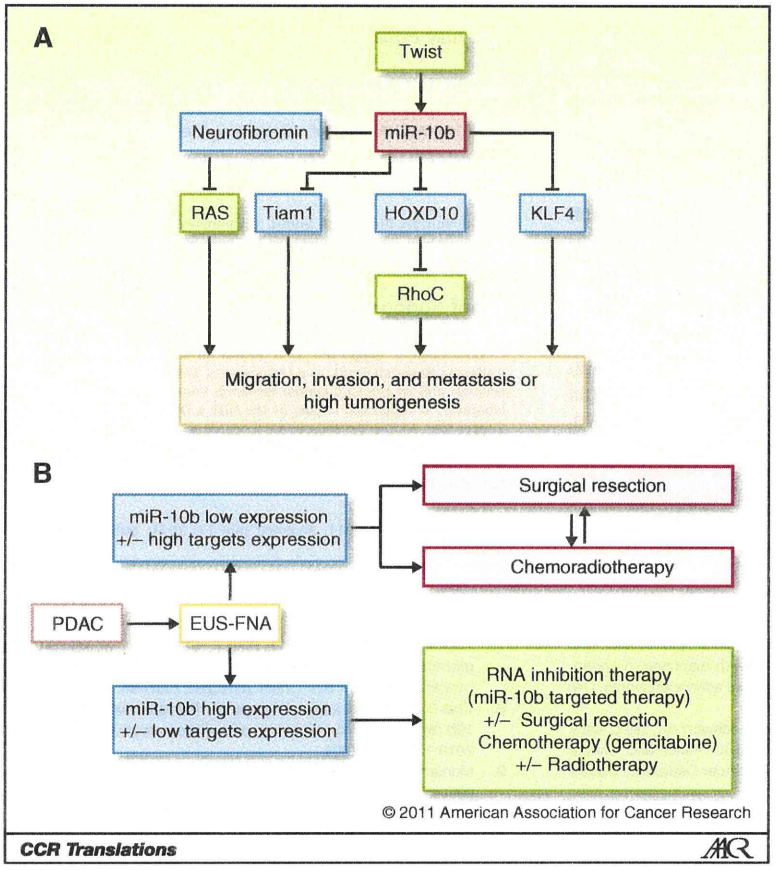

Figure 1. Possible future PDAC management decisions using ISH of miR-10b expression. A, molecular mechanism of miR-10b action; B, treatment decisions based on miR-10b and target expression.

spatial cancer-specific expression of miR-10b. Another method that can select only cancer cells, laser capture microdissection (11), is more time consuming and technically demanding than the combination of ISH and immunohistochemical analysis.

Finally, and most significantly, these authors' findings have high translation potential. They initially determined the expression of miR-10b, miR-21, miR-155, miR-196a, and miR-210 using ISH in 10 resected PDAC formalin-fixed, paraffin-embedded clinical specimens and 3 non-cancerous tissues. The authors found that miR-10b was the most frequently and consistently upregulated in cancer cells. They then used ISH to determine miR-10b expression in 95 PDAC and 11 benign EUS-FNA biopsy samples. In cancer tissue, miR-10b expression (measured automatically as mean fluorescence intensity) was about 5 times higher than that in benign tissue. miR-10b expression was significantly useful for cancer diagnosis. Subsequently, they compared miR-10b expression and the response of neoadjuvant chemoradiotherapy. They found significantly lower miR-10b levels in tumors that responded than in those that did not. In addition, they detected significantly lower miR-10b levels in resectable than in unresectable tumors. These findings indicate that miR-10b can be used to predict response to therapy. Thereafter, the authors found a significantly longer time to metastasis in patients with low miR-10b expression. Moreover, patients with low miR-10b expression had longer overall survival durations than did patients with high expression, for all stages; durations were even longer for stages I and II. These results suggest that miR-10b could be predictive of prognosis. It is clear that further studies to identify the critical targets of miR-10b in pancreatic cancer will also identify other pathways to target, either alone or in combination with chemotherapy.

One of the most significant findings of this study is the value of miR-10b for use in therapeutic decision making (Fig. 1B). Preis and colleagues (1) found that patients with low miR-10b expression experienced relatively better responses to gemcitabine-based neoadjuvant therapy and better prognoses. The best treatment for patients with unfavorably high miR-10b expression will be the most difficult decision in clinical practice. New alternative therapies, including miR-10b–targeted therapy, are needed. Many miRNAs have been reported to be oncogenic or suppressive, but few *in vivo* therapeutic advances have been made. Researchers have evaluated the use of

Published OnlineFirst August 4, 2011; DOI:10.1158/1078-0432.CCR-11-1477

antagomirs as *in vivo* miRNA antagonists; antagomirs are a type of chemically engineered, cholesterol-conjugated antisense RNA oligonucleotide (12). A miR-10b antagomir was evaluated in a 4T1 mouse mammary tumor metastasis model. Ma and colleagues found that antagomir-10b prevents metastatic dissemination of cancer cells from the primary tumor but does not affect late stages of the metastatic process, when tumor cells have disseminated (12).

An important question is whether detection of miR-10b expression by ISH is ready for use in clinical practice. This study was done at a single institution and was retrospective; its findings must be confirmed in a multi-institutional prospective clinical trial. Clearly, cooperation and support among clinical surgeons, oncologists, pathologists, and molecular scientists is essential. miRNA detection with combined ISH and immunohistochemical staining could be challenging when the miRNAs are not well expressed. Furthermore, staining for the expression characterization of known target genes, in addition to specific miRNAs, could improve prediction accuracy (Fig. 1B). If the findings of this study are confirmed, they will be of great help toward developing a clinical strategy to select PDAC patients who will experience a response to neoadjuvant therapy and may experience a better outcome.

Disclosure of Potential Conflicts of Interest

No potential conflicts of interest were disclosed.

Acknowledgments

The authors thank Ann Sutton (Department of Scientific Publications, MD Anderson Cancer Center) for her help with the editing of this manuscript.

Grant Support

G.A. Calin is supported as a Fellow of the University of Texas MD Anderson Research Trust, as a University of Texas System Regents Research Scholar, and by the CLL Global Research Foundation. Work in Dr. Calin's laboratory is supported in part by the NIH; a Department of Defense Breast Cancer Idea Award; developmental research awards in Breast Cancer, Ovarian Cancer, Brain Cancer, Multiple Myeloma, and Leukemia SPOREs; a 2009 Seena Magowitz–Pancreatic Cancer Action Network AACR Pilot Grant; and the Arnold Foundation.

Received July 7, 2011; accepted July 21, 2011; published OnlineFirst August 4, 2011.

References

1. Preis M, Gardner TB, Gordon SR, Pipas MJ, Mackenzie TA, Klein EE, et al. microRNA-10b expression correlates with response to neoadjuvant therapy and survival in pancreatic ductal adenocarcinoma. Clin Cancer Res 2011;17:5812–21.
2. Bilimoria KY, Bentrem DJ, Ko CY, Ritchey J, Stewart AK, Winchester DP, et al. Validation of the 6th edition AJCC Pancreatic Cancer Staging System: report from the National Cancer Database. Cancer 2007;110:738–44.
3. Locker GY, Hamilton S, Harris J, Jessup JM, Kemeny N, Macdonald JS, et al. ASCO. ASCO 2006 update of recommendations for the use of tumor markers in gastrointestinal cancer. J Clin Oncol 2006;24:5313–27.
4. Nicoloso MS, Spizzo R, Shimizu M, Rossi S, Calin GA. MicroRNAs—the micro steering wheel of tumour metastases. Nat Rev Cancer 2009;9:293–302.
5. Calin GA, Croce CM. MicroRNAs and chromosomal abnormalities in cancer cells. Oncogene 2006;25:6202–10.
6. Ma L, Teruya-Feldstein J, Weinberg RA. Tumour invasion and metastasis initiated by microRNA-10b in breast cancer. Nature 2007;449:682–8.
7. Tian Y, Luo A, Cai Y, Su Q, Ding F, Chen H, et al. MicroRNA-10b promotes migration and invasion through KLF4 in human esophageal cancer cell lines. J Biol Chem 2010;285:7986–94.
8. Chai G, Liu N, Ma J, Li H, Oblinger JL, Prahalad AK, et al. MicroRNA-10b regulates tumorigenesis in neurofibromatosis type 1. Cancer Sci 2010;101:1997–2004.
9. Moriarty CH, Pursell B, Mercurio AM. miR-10b targets Tiam1: implications for Rac activation and carcinoma migration. J Biol Chem 2010;285:20541–6.
10. Eloubeidi MA, Chen VK, Eltoum IA, Jhala D, Chhieng DC, Jhala N, et al. Endoscopic ultrasound-guided fine needle aspiration biopsy of patients with suspected pancreatic cancer: diagnostic accuracy and acute and 30-day complications. Am J Gastroenterol 2003;98:2663–8.
11. Fujita H, Ohuchida K, Mizumoto K, Itaba S, Ito T, Nakata K, et al. High EGFR mRNA expression is a prognostic factor for reduced survival in pancreatic cancer after gemcitabine-based adjuvant chemotherapy. Int J Oncol 2011;38:629–41.
12. Ma L, Reinhardt F, Pan E, Soutschek J, Bhat B, Marcusson EG, et al. Therapeutic silencing of miR-10b inhibits metastasis in a mouse mammary tumor model. Nat Biotechnol 2010;28:341–7.

Ann Surg Oncol (2012) 19:2066–2071
DOI 10.1245/s10434-011-2024-5

Annals of
SURGICAL ONCOLOGY
OFFICIAL JOURNAL OF THE SOCIETY OF SURGICAL ONCOLOGY

ORIGINAL ARTICLE – TRANSLATIONAL RESEARCH AND BIOMARKERS

Clinicopathological Significance of BMP7 Expression in Esophageal Squamous Cell Carcinoma

Koichi Megumi, MD, Sumiya Ishigami, MD, Yasuto Uchikado, MD, Yoshiaki Kita, MD, Hiroshi Okumura, MD, Masataka Matsumoto, MD, Yoshikazu Uenosono, MD, Takaaki Arigami, MD, Yuko Kijima, MD, Masaki Kitazono, MD, Hiroyuki Shinchi, MD, Shinichi Ueno, MD, and Shoji Natsugoe, MD

Department of Surgical Oncology, Digestive Surgery, Kagoshima University, Graduate School of Medicine, Kagoshima, Japan

ABSTRACT

Background. Bone morphogenetic proteins (BMPs) are secreted signaling molecules belonging to the transforming growth factor-β (TGF-β) superfamily of growth factors. Recent studies have shown that the influence of the expression of BMP7 was altered in several tumors. The purpose of the current study was to examine the expression of BMP7 in esophageal squamous cell carcinoma and to clarify the clinical impact of BMP7 expression in esophageal squamous cell carcinoma (ESCC).

Methods. A total of 180 patients with ESCC who underwent surgical resection from 1991 to 2004 were eligible for this study. The expression of BMP7 in esophageal tumor tissues was examined immunohistochemically.

Results. BMP7 expression was found in the cytoplasm of cancer cells. BMP7 positivity was observed in 61.7% of tumors. The BMP7-positive group had deeper progression, more advanced stages, and greater venous invasion than those without BMP7 expression ($p < 0.001$, $p < 0.005$, and $p < 0.0005$, respectively). In addition, expression of BMP7 correlated with poorer prognosis ($p < 0.0005$). Multivariate analysis showed that BMP7 expression status was an independent prognostic factor ($p < 0.05$).

Conclusions. Patients with expression of BMP7 in ESCC had high malignant potential. BMP7 could be a useful prognostic marker for patients with ESCC.

First Received: 14 December 2010;
Published Online: 13 September 2011

K. Megumi, MD
e-mail: aircarter@goo.jp

Esophageal squamous cell carcinoma (ESCC) is aggressive in gastrointestinal tract carcinomas. Even when patients with ESCC undergo curative resection, postoperative relapse often occurs. Attempts to evaluate the group at high risk of recurrence have been made in respect to tumor aggressiveness. The tumor behavior of ESCC at the molecular level has been intensively analyzed.

Among the molecular factors available for possible evaluation of tumor aggressiveness, bone morphogenetic protein (BMP) is a member of the transforming growth factor (TGF)-β superfamily known to regulate cell proliferation, apoptosis, and differentiation during human development.[1,2] BMPs bind cell membrane type I and type II receptors of serine/threonine kinases, eliciting intracellular signaling via Smad1, 5, 8, and 9 proteins.[3,4] Recent studies have shown that BMP7 maintains epithelial and endothelial phenotypes against epithelial-mesenchymal transition (EMT).[5,6]

BMP7 is present in cancers, including breast, prostate, and colon cancers, in which it is implicated in regulating cancer cell proliferation.[7–9] Overexpression of BMP7 mRNA in colorectal cancer patients was significantly associated with poor prognosis and low overall survival.[10] However, the expression of BMP7 in ESCC has not been evaluated.

In the present study, the BMP7 expression in surgical specimens of ESCC was examined to evaluate whether this molecule is useful to predict postoperative outcome.

MATERIALS AND METHODS

Patients and Specimens

There were 180 patients diagnosed with ESCC (163 males and 17 females) who underwent R0

esophagectomy with lymph node dissection between 1991 and 2004 at Kagoshima University Hospital, Kagoshima, Japan. The median age of the patients was 65.2 (range, 39–84) years.

None of these patients underwent endoscopic mucosal resection, preoperative chemotherapy or radiotherapy, or had metachronous multiple cancer in other organs. Specimens of cancer tissue and noncancerous adjacent tissue were collected from patients after informed consent had been obtained in accordance with the institutional guidelines of our hospital. Using TNM classification of the International Union Against Cancer,[11] all of the M1 tumors exhibited distant lymph node metastases. All patients were followed-up after discharge, with x-ray examination and tumor marker assays (squamous cell carcinoma antigen and carcinoembryonic antigen) performed every 1 to 3 months, computed tomography every 3 to 6 months, and ultrasonography every 6 months. Bronchoscopy and endoscopy were performed if necessary.

Postoperative follow-up data were obtained from all patients, with a median follow-up period of 39 (range, 1–137) months. According to TNM classification, 74 of the 180 patients had T1 tumors, 25 patients had T2 tumors, 78 patients had T3 tumors, and 3 patients had T4 tumors.

Immunohistochemical Staining and Evaluation of BMP7 in ESCC

Tumor samples were fixed with 10% formaldehyde in phosphate-buffered saline (PBS), embedded in paraffin, and sectioned into 4-μm-thick slices. They were deparaffinized in xylene and dehydrated with a series of graded ethanol. The endogenous peroxidase activity of specimens was blocked by immersing the slides in a 3% hydrogen peroxidase-methanol solution for 10 min at room temperature. After washing three times with PBS for 5 min each, the sections were treated with 1% bovine serum albumin for 30 min to block nonspecific reactions at room temperature. Then, the sections were incubated with primary antibody to BMP7 (1:200 R&D System) at 4°C overnight and subsequently stained with secondary antibodies for 30 min. The sections were incubated with avidin–biotin complex for 60 min, and reactions were visualized using diaminobenzidine tetrahydrochloride for 2 min. The sections were rinsed briefly in water and counterstained with hematoxylin for 30 s. Normal human kidney was used as a positive (medullary rays) and negative (glomeruli) control to verify both BMP7 antibody specificity and staining quality (Fig. 1a).[12] Immunohistochemistry was independently evaluated by two investigators (KM and SI) who

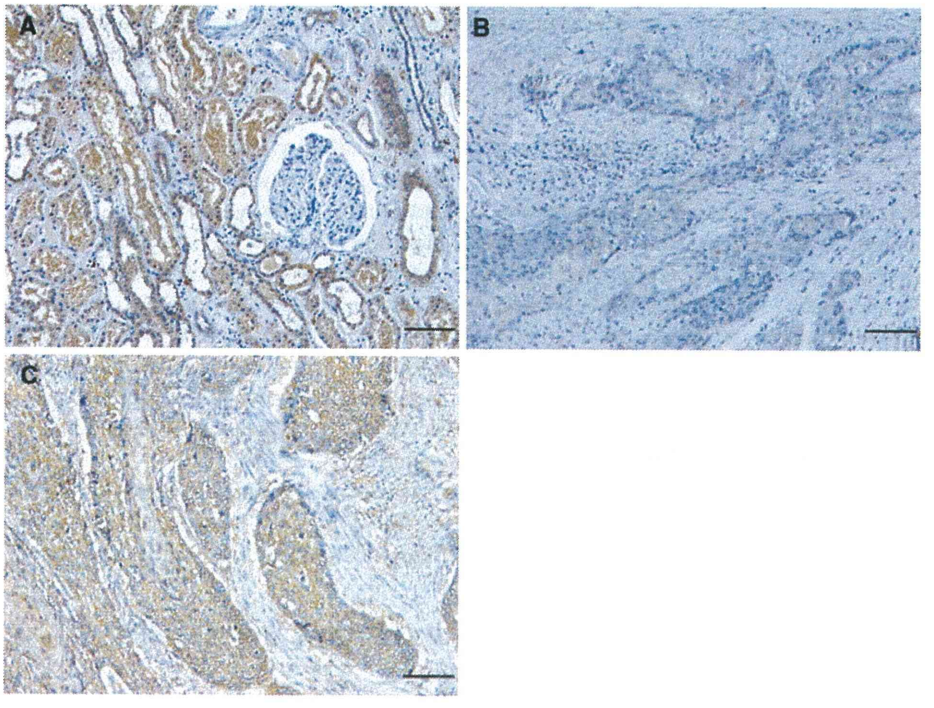

FIG. 1 Normal kidney section as a positive control for BMP7 staining. **a** BMP7 expression was seen in medullary rays and not seen in glomeruli (×200). Expression of BMP7 in ESCCs. **b** Negative expression of BMP7 (×200). **c** Positive expression of BMP7 was detectable in cytoplasm and membranes (×200). *Scale bar* 100 μm

had no information about the patients' clinical data. In cases in which the immunohistochemical evaluation of the two observers differed, slides were evaluated by a third observer (SN).

To evaluate the expression of BMP7, ten fields (within the tumor and at the invasive front) were selected and expression in 1,000 tumor cells (100 cells/field) was evaluated using high-power (×200) microscopy. Expression of BMP7 was assessed using the proportion of positive cells and using intensity. At first, we classified each sample into one of three categories in terms of the proportion of positive cells: 1+, 0–29%; 2+, 30–59%; and 3+, ≥60% positive cells. In addition, we classified each sample into one of three categories according to the intensity: 1+, weak; 2+, moderate; and 3+, strong. The tumors with strong staining at least 30% of the cells and moderate staining at least 60% of the cells were considered BMP7-positive. We used this evaluation because of the heterogeneity of the ESCC samples and the fact that the deeper the tumors invaded, the stronger their intensity tended to become. We improved the evaluation method used by Liu et al.[13]

Statistical Analysis

Statistical analysis of group differences was performed using the χ^2 test. The Kaplan-Meier method was used for survival analysis, and differences in survival were estimated by using the log-rank test. Prognostic factors were examined by univariate and multivariate analyses (Cox proportional hazards regression model). A p value <0.05 was considered to indicate statistical significance. All statistical analyses were performed using the StatView for Windows software (Version 5.0, Abacus Concepts, Berkeley, CA).

RESULTS

BMP7 Expression of ESCC

BMP7 expression was identified in cellular membrane and cytoplasm of ESCC and was detected rarely in normal esophageal epithelium. Positivity of BMP7 expression was seen in 111 (61.7%) of 180 patients (Fig. 1c).

Relationship Between BMP7 Expression and Clinicopathological Features

High-intensity BMP7 expression was detected more at deeper areas in ESCC. The correlations between BMP7 expression and clinicopathological characteristics are shown in Table 1. The BMP7-positive group had significantly deeper tumor invasion ($p < 0.001$), more advanced stages ($p = 0.0012$), more venous invasion ($p = 0.0002$), and more locoregional recurrence ($p = 0.027$) than the BMP7-negative group. We had 23 locoregional recurrences during the period of this study: 3 were surgical anastomosis recurrences, and 20 were lymph node recurrences. Furthermore, we examined the relationship between BMP7 expression and locoregional recurrence; 19 of 23 patients with locoregional recurrence had BMP7-positive expression (Table 2).

TABLE 1 Relationship between BMP7 expression and clinicopathologic findings

	BMP7 expression		p
	(−) $n = 69$	(+) $n = 111$	
Total ($N = 180$)			
Age (mean ± SD)	64.6 ± 9	65.6 ± 9	0.975
Gender			
Male	65	98	0.178
Female	4	13	
Histology			
Well	19	36	0.588
Moderate	34	53	
Poor	9	22	
p^T			
T1	36	23	<0.0001
T2, T3, T4	33	88	
p^N			
N0	34	43	0.171
N1	35	68	
p^M			
M0	55	78	0.06
M1	14	33	
Lymphatic invasion			
Negative	24	24	0.052
Positive	45	87	
Venous invasion			
Negative	40	33	0.0002
Positive	29	78	
Stage			
I	20	13	0.0012
IIA, IIB	25	28	
III	10	37	
IV	14	33	
Locoregional recurrence			
Negative	65	4	0.027
Positive	92	19	

SD standard deviation

TABLE 2 Relationship between immunohistochemical staining for BMP7 expression and locoregional recurrence

Recurrence site	Total	BMP7 expression	
		Positive ($n = 19$)	Negative ($n = 4$)
Lymph nodes	20	17 (85%)	3 (15%)
Surgical anastomosis	3	2 (66%)	1 (33%)

BMP7 Expression and Patients' Survival

The 5-year overall survival rate was significantly lower in patients with BMP7-positive expression than in those with negative expression ($p = 0.0004$; Fig. 2a). In 77 patients who had no lymph node metastasis, 43 patients with BMP7-positive expression also had significantly lower 5-year overall survival rate than that of patients judged to have BMP7-negative expression ($p = 0.0016$; Fig. 2b).

Univariate and Multivariate Analysis of Survival

Table 3 shows the results of univariate and multivariate analyses of the factors related to patient prognosis. Univariate regression analyses revealed that depth of tumor invasion, lymph node metastasis, pM status (distant lymph node metastasis), venous invasion, locoregional recurrence, and BMP7 expression significantly affected postoperative outcome. Multivariate analysis indicated that BMP7 expression was one of the independent prognostic factors ($p = 0.046$), along with the depth of invasion ($p = 0.019$), and pM status (distant lymph node metastasis) ($p = 0.009$; Table 3).

DISCUSSION

This is the first report to show an association between BMP7 expression and clinicopathological findings in ESCC. BMP7 positivity was observed in 61.7% of ESCC tumors, which was a higher incidence than in colorectal (41%) and breast cancers (46%).[10,14]

BMP7 expression have been reported to be involved in the growth of several cancer cells, such as osteosarcoma, malignant melanoma, prostate cancer, breast cancer, renal cell cancer, colorectal cancer, and gastric cancer, causing increased aggression or suppression.[10,15–20] We showed that BMP7 expression in ESCC was significantly associated with the tumor depth, stages, and venous invasion. Motoyama et al. investigated BMP7 mRNA in colorectal cancer and showed its significant association with tumor extension and liver metastasis.[10] Aoki et al. reported immunohistochemical expression of BMP7 in gastric cancer was significantly related to the depth of tumors, nodal involvement, lymphatic invasion, and venous invasion.[20] Those findings agree with our results. In this context, cancerous BMP7 positivity may reflect tumor aggressiveness.

In contrast, Kwak et al. reported that cancerous BMP7 expression correlated with better surgical outcome in renal cell carcinoma.[15] Renal cells are used as a positive control of BMP7 expression; this contradictory finding supports organ-specificity. Aoki et al. also reported that BMP7 expression in gastric cancer was significantly higher in the well- and moderately differentiated histological group than in the poorly differentiated histological group. In contrast, in this study, we showed no relationship between BMP7 expression and tumor histological type; this contradictory findings supports tumor-specificity (histologic differences between squamous cell carcinoma and adenocarcinoma).

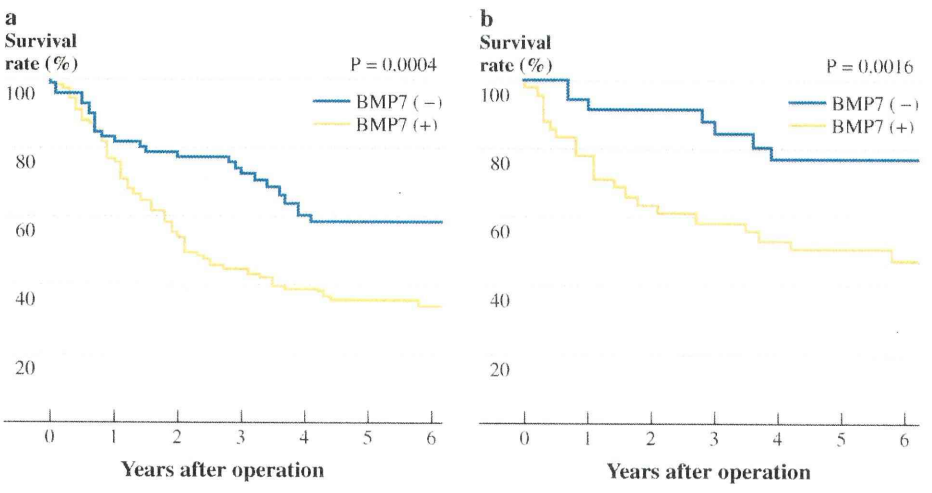

FIG. 2 **a** Overall 5-year survival curves of patients with esophageal cancer according to the expression of BMP7. Patients who were positive for BMP7 expression exhibited significantly poorer prognosis than those negative for BMP7 expression. **b** Overall 5-year survival curves of patients without lymph node metastasis in relation to BMP7 expression. Patients who were positive for BMP7 expression exhibited significantly poorer prognosis than those negative for BMP7 expression

TABLE 3 Univariate and multivariate analysis of prognostic factors in ESCC

Factors	Univariate analysis	Multivariate analysis		
	p	*p*	Hazard ratio	95% CI
pT (1/2,3,4) (negative/positive)	<0.0001*	0.019*	1.89	1.107–3.225
pN (negative/positive)	0.0003*	0.377	1.269	0.748–2.15
Venous invasion (negative/positive)	0.006*	0.622	1.121	0.71–1.769
pM (negative/positive)	<0.0001*	0.009*	1.93	1.177–3.164
Locoregional recurrence (negative/positive)	0.03*	0.587	1.162	0.673–2.008
BMP7 expression	0.0004*	0.046*	1.61	1.008–2.576

* $p < 0.05$

BMP7 expression by immunohistochemistry was significantly associated with lower recurrence-free survival in malignant melanoma and breast cancer.[14,17] Our recent study showed BMP7 expression was significantly related to the locoregional recurrence. Those who had BMP7 expression tended to occur local lymph node relapse. Those findings might have important clinical significance. To determinate BMP7 expression status in primary ESCC could help to identify patients who are at high risk to develop early local lymph node recurrence.

In vitro, the BMP7 signaling pathway in malignant tumors has not been fully understood. From our results, in ESCC, these specific signals for BMP7 may correspond with tumor invasion in those signals that BMP7 stimulates.

In many cancers, TGF-β is a protumorigenic factor that stimulates EMT.[21–23] In contrast, BMP7 is a strong inducer of the reverse process (mesenchymal-epithelial transition; MET) during embryonic development.[24–26] Moreover, BMP7 can inhibit TGF-β-induced fibrosis and counteracts TGF-β-induced EMT in normal renal epithelial cells.[27–29] In contrast, in this study, overexpression of BMP7 in ESCC was significantly related to tumor aggressiveness. BMP7 might be related to tumor migration ability in ESCC. We need to find out more details about the cross-talk between BMP7 and TGF-β signaling pathways in the context of EMT.

As a prognostic parameter, Aoki et al. reported that immunohistochemical BMP7 expression in gastric cancer patients was associated with poor overall survival.[20] Moreover, overexpression of BMP7 mRNA was significantly associated with lower overall survival in colorectal cancer.[10]

In this study, concerning the overall survival analysis, tumor depth, lymph node metastasis, venous invasion, distant lymph node metastasis, locoregional recurrence, and BMP7 expression were prognostic factors on univariate analysis. We showed that BMP7 expression was one of independent prognostic factors, along with tumor depth, and distant lymph node metastasis on multivariate analysis in accordance with results for other digestive tract cancers. BMP7 expression could be used as a useful prognostic parameter predicting the survival of postoperative ESCC patients.

Various molecular markers have been shown to be associated with development and progression of ESCC, including cyclin D1, smad4, Fas, cyclin B1, CD151, Bmi-1, and osteopontin.[13,30–35] Naitoh et al. demonstrated that the survival rate for the patients with overexpression of cyclin D1 was very low even in the patients without lymph node metastasis.[30] In this study, the 5-year overall survival rate for the patients with BMP7 positive expression was significantly worse than those with negative expression even in the patients without lymph node metastasis. BMP7 expression may be a useful marker for high-risk patients of ESCC without lymph node metastasis. This enables us to choose postoperative treatment, including chemotherapy.

Moreover, we showed that BMP7 expression tends to correlate with lymphatic invasion ($p = 0.052$). Thus, cancerous BMP7 expression in a biopsy may be informative to predict lymphatic invasion. When selecting whether to perform endoscopic resection for early ESCC, we can use cancerous BMP7 expression as a predictor of lymphatic invasion.

In conclusion, BMP7 expression in ESCC plays a critical role in tumor proliferation and invasion. Expression of BMP7 may be a predictor of poor overall survival. This independent molecular marker for high-risk patients could help us in our attempts to individualize patients' therapy.

REFERENCES

1. Patel SR, Dressler GR. BMP7 signaling in renal development and disease. *Trends Mol Med.* 2005;11:512–8.
2. Milan M. Sculpting a fly leg: BMP boundaries and cell death. *Nat Cell Biol.* 2007;9:17–8.
3. Attisano L, Wrana JL. Signal transduction by the TGF-beta superfamily. *Science.* 2002;296:1646–7.

4. Massague J, Seoane J, Wotton D. Smad transcription factors. *Genes Dev.* 2005;19:2783–810.
5. Buijs JT, Rentsch CA, van der Horst G, et al. BMP7, a putative regulator of epithelial homeostasis in the human prostate, is a potent inhibitor of prostate cancer bone metastasis in vivo. *Am J Pathol.* 2007;171:1047–57.
6. Zeisberg EM, Tarnavski O, Zeisberg M, et al. Endothelial-to-mesenchymal transition contributes to cardiac fibrosis. *Nature.* 2007;13:952–61.
7. Alamo EL, Rauta J, Kallioniemi A, et al. Bone morphogenetic protein 7 is widely overexpressed in primary breast cancer. *Genes Chromosomes Cancer.* 2006;45:411–9.
8. Miyazaki H, Watabe T, Kitamura T, Miyazono K. BMP signals inhibit proliferation and in vivo tumor growth of androgen-insensitive prostate carcinoma cells. *Oncogene.* 2004;23: 9326–35.
9. Beck SE, Jung BH, Del Rosario E, Gomez J, Carethers JM. BMP-induced growth suppression in colon cancer cells is mediated by p21(WAF1) stabilization and modulated by RAS/ERK. *Cell Signal.* 2007;19:1465–72.
10. Motoyama K, Tanaka F, Kosaka Y, et al. Clinical significance of BMP7 in human colorectal cancer. *Ann Surg Oncol.* 2008;15: 1530–36.
11. Sobin LH, Fleming ID. TNM classification of malignant tumors. 5th ed. Union Internationale Contre le Cancer and the American Joint Committee on Cancer. *Cancer.* 1997;80:1803–4.
12. Wang SN, Lapage J, Hirschberg R. Loss of tubular bone morphogenetic protein-7 in diabetic nephropathy. *J Am Soc Nephrol.* 2001;12:2392–9.
13. Liu WI, Guo XZ, Zeng MS, et al. Prognostic relevance of Bmi-1 expression and autoantibodies in esophageal squamous cell carcinoma. *BMC Cancer.* 2010;10:467.
14. Alarmo EL, Korhonen T, Huhtala H, et al. Bone morphogenetic protein 7 expression associates with bone metastasis in breast carcinomas. *Ann Oncol.* 2008;19:308–14.
15. Kwak C, Park YH, Kim IY, et al. Expression of bone morphogenetic proteins, the subfamily of the transforming growth factor-β superfamily, in renal cell carcinoma. *J Urol.* 2007;178:1062–7.
16. Sulzbacher I, Birner P, Lang S, et al. The expression of bone morphogenetic proteins in osteosarcoma and its relevance as a prognostic parameter. *J Clin Pathol.* 2002;55:381–5.
17. Rothhammer T, Wild PJ, Bosserhoff AK, et al. Bone morphogenetic protein 7 (BMP7) expression is a potential novel prognostic marker for recurrence in patients with primary melanoma. *Cancer Biomark.* 2007;3:111-7.
18. Masuda H, Hukabori Y, Yamanaka H, et al. Expression of bone morphogenetic protein-7 (BMp-7) in human prostate. *Prostate.* 2004;59:101–6.
19. Alamo EL, Rauta J, Kallioniemi A, et al. Bone morphogenetic protein 7 is widely overexpressed in primary breast cancer. *Genes Chromosomes Cancer.* 2006;45:411–9.
20. Aoki M, Ishigami S, Natugoe S, et al. Expression of BMP-7 in human gastric cancer and its clinical significance. *Br J Cancer.* 2011;104:714–8.
21. Thiery JP. Epithelial-mesenchymal transitions in tumour progression. *Nat Rev Cancer.* 2002;2:442–54.
22. Peinado H, Quintanilla M, Cano A. Transforming growth factor beta-1 induces snail transcription factor in epithelial cell lines: mechanisms for epithelial mesenchymal transitions. *J Biol Chem.* 2003;278:21113–23.
23. Piek E, Moustakas A, Kurisaki A, et al. TGF-(beta) type I receptor/ALK-5 and Smad proteins mediate epithelial to mesenchymal transdifferentiation in NMuMG breast epithelial cells. *J Cell Sci.* 1999;112:4557–68.
24. Dudley AT, Lyons KM, Robertson EJ. A requirement for bone morphogenetic protein-7 during development of the mammalian kidney and eye. *Genes Dev.* 1995;9:2795–807.
25. Luo G, Hofmann C, Bronckers AL, et al. BMP-7 is an inducer of nephrogenesis, and is also required for eye development and skeletal patterning. *Genes Dev.* 1995;9:2808–20.
26. Vukicevic S, Kopp JB, Luyten FP, et al. Induction of nephrogenic mesenchyme by osteogenic protein 1 (bone morphogenetic protein 7). *Proc Natl Acad Sci U S A* 1996;93:9021–6.
27. Simic P, Vukicevic S. Bone morphogenetic proteins in development and homeostasis of kidney. *Cytokine Growth Factor Rev.* 2005;16:299–308.
28. Wang S, Hirschberg R. BMP7 antagonizes TGF-beta-dependent fibrogenesis in mesangial cells. *Am J Physiol Renal Physiol.* 2003;284:F1006–13.
29. Zeisberg M, Hanai J, Sugimoto H, et al. BMP-7 counteracts TGF-beta1-induced epithelial-to-mesenchymal transition and reverses chronic renal injury. *Nature.* 2003;9:964–8.
30. Naitoh H, Shibata J, Hattori T, et al. Overexpression and localization of cyclin D1 mRNA and antigen in esophageal cancer. *Am J Pathol.* 1995;5:1161–9.
31. Natsugoe S, Xiangming C, Aikou T, et al. Smad4 and transforming growth factor β1 expression in patients with squamous cell carcinoma of the esophagus. *Clin Cancer Res.* 2002;8: 1838–42.
32. Chan KW, Lee PY, Srivastava G, et al. Clinical relevance of Fas expression in oesophageal squamous cell carcinoma. *J Clin Pathol.* 2006;59:101–4.
33. Takeno S, Noguchi T, Műller W, et al. Prognostic value of cyclin B1 in patients with esophageal squamous cell carcinoma. *Cancer.* 2002;94:2874–81.
34. Suzuki S, Miyazaki T, Kuwano H, et al. Prognostic significance of CD151 expression in esophageal squamous cell carcinoma with aggressive cell proliferation and invasiveness. *Ann Surg Oncol.* 2011;18:888–93.
35. Kita Y, Natsugoe S, Aikou T, et al. Expression of osteopontin in oesophageal squamous cell carcinoma. *Br J Cancer.* 2006;95: 634–8.

Thrombosis Research xxx (2011) xxx–xxx

Contents lists available at SciVerse ScienceDirect

Thrombosis Research

journal homepage: www.elsevier.com/locate/thromres

Regular Article

Heparin modulates the conformation and signaling of platelet integrin αIIbβ3

Mayumi Yagi [a,*], Jacqueline Murray [a,b], Kurt Strand [a], Scott Blystone [c], Gianluca Interlandi [d], Yasuo Suda [e], Michael Sobel [a,b]

[a] Research & Development, Veterans Affairs Puget Sound Health Care System, Seattle, WA
[b] Division of Vascular Surgery, Department of Surgery, University of Washington, Seattle, WA
[c] Department of Cell and Developmental Biology, SUNY Upstate Medical University, Syracuse, NY
[d] Department of Bioengineering, University of Washington, Seattle, WA
[e] Department of Nanostructure and Advanced Materials, Graduate School of Science and Engineering, Kagoshima University, Kagoshima, Japan

ARTICLE INFO

Article history:
Received 26 August 2011
Received in revised form 7 November 2011
Accepted 30 November 2011
Available online xxxx

Keywords:
Heparin
Integrin αIIbβ3 (platelet glycoprotein IIbIIIa)
Platelet activation
Src kinase
Surface plasmon resonance
Tyrosine phosphorylation

ABSTRACT

Introduction: The glycosaminoglycan heparin has been shown to bind to platelet integrin αIIbβ3 and induce platelet activation and aggregation, although the relationship between binding and activation is unclear. We analyzed the interaction of heparin and αIIbβ3 in detail, to obtain a better understanding of the mechanism by which heparin acts on platelets.
Methods: We assessed conformational changes in αIIbβ3 by flow cytometry of platelets exposed to unfractionated heparin. In human platelets and K562 cells engineered to express αIIbβ3, we assayed the effect of heparin on key steps in integrin signaling: phosphorylation of the β3 chain cytoplasmic tail, and activation of src kinase. We measured the heparin binding affinity of purified αIIbβ3, and of recombinant fragments of αIIb and β3, by surface plasmon resonance.
Results and conclusions: Heparin binding results in conformational changes in αIIbβ3, similar to those observed upon ligand binding. Heparin binding alone is not sufficient to induce tyrosine phosphorylation of the integrin β3 cytoplasmic domain, but the presence of heparin increased both β3 phosphorylation and src kinase activation in response to ligand binding. Specific recombinant fragments derived from αIIb bound heparin, while recombinant β3 did not bind. This pattern of heparin binding, compared to the crystal structure of αIIbβ3, suggests that heparin-binding sites are located in clusters of basic amino acids in the headpiece and/or leg domains of αIIb. Binding of heparin to these clusters may stabilize the transition of αIIbβ3 to an open conformation with enhanced affinity for ligand, facilitating outside-in signaling and platelet activation.

Published by Elsevier Ltd.

Introduction

The glycosaminoglycan heparin is a potent anticoagulant that is extensively used in the prevention and treatment of cardiovascular disorders. However, the efficacy of heparin is limited in part by its effect on platelets. Patients receiving intravenous heparin commonly experience an immediate, transient but mild non-immune-mediated thrombocytopenia, associated with biochemical evidence of platelet activation [1–5]. Heparin-mediated platelet activation should be distinguished from the much rarer syndrome of heparin-induced thrombocytopenia, caused by the formation of antibodies to platelet factor 4 (PF4) in a complex with heparin [1]. Both in vivo and in vitro, unfractionated heparin appears to be a stronger stimulant of platelet activation than lower molecular weight heparins [6–10]. In previous work, we have characterized the heparin oligosaccharide that binds to platelets, and shown that heparin binds to platelet integrin αIIbβ3 (platelet glycoprotein IIbIIIa) [11–15]. Thus, it seems likely that heparin binding to αIIbβ3 is directly related to its stimulatory effects. Understanding the interaction of heparin with platelets will help in the development of safer anticoagulants.

Integrin αIIbβ3 is the major platelet surface receptor for fibrinogen and other RGD-containing proteins. Like other integrins, αIIbβ3 is a bidirectional receptor that undergoes conformational changes and induces intracellular signaling upon ligand engagement (outside-in signaling), as well as upon cell activation by soluble such as thrombin or ADP (inside-out signaling). Both processes contribute to a signaling cascade that ultimately results in profound morphological and biochemical changes in the platelet [16,17]. One of the first steps in this cascade is tyrosine phosphorylation of the integrin β3 cytoplasmic tail, which alters its association with the platelet

Abbreviations: GlcNS6S-IdoA2S, glucosamine N-sulfate (6-O-sulfate)-iduronic acid (2-O-sulfate); mAb, monoclonal antibody; PBS, phosphate-buffered saline; PRP, platelet-rich plasma; pY, phosphotyrosine; SPR, surface plasmon resonance.

* Corresponding author at: Research & Development (151), Seattle Division, VA Puget Sound Health Care System, 1660 South Columbian Way, Seattle, 98108. Tel.: +1 206 277 1188; fax: +1 206 277 4483.
E-mail address: myagi@uw.edu (M. Yagi).

0049-3848/$ – see front matter. Published by Elsevier Ltd.
doi:10.1016/j.thromres.2011.11.054

cytoskeleton, leading to shape changes, and ultimately to aggregation and release of mediators contained in platelet α granules [18].

Recent evidence indicates that heparin augments the ligand-induced phosphorylation of platelet cytoplasmic proteins involved in multiple signal transduction pathways, including through integrin αIIbβ3 [19]. In the work presented here, we show that heparin directly amplifies signaling through integrin αIIbβ3. Our experiments show that heparin augments ligand-induced conformational changes in αIIbβ3, as well as increasing tyrosine phosphorylation of both the integrin β3 cytoplasmic domain and associated src kinase. In addition, we map the binding sites of heparin on the αIIbβ3 molecule. Our results indicate that heparin-induced platelet activation is caused by the binding of heparin to αIIbβ3, with induction or stabilization of a more activated conformation. We find that heparin binds predominantly to the αIIb subunit, and suggest some potential heparin-binding sites within the receptor.

Materials and methods

Detailed procedures and additional figures are included in the Supporting Information for this paper. For all experiments, we used a standard unfractionated porcine mucosal heparin (Celsus, Inc., M.W. ~15,000 Da, 179 units/mg).

Flow cytometry of integrin activation

All blood samples were collected from normal volunteers after obtaining informed consent following protocols approved by the Institutional Review Board. Whole blood was collected into Vacutainers containing 3.2% buffered sodium citrate (Becton-Dickinson) and immediately centrifuged to obtain platelet-rich plasma (PRP). PRP was incubated with PBS, heparin (Celsus, 5 μg/ml final concentration), EDTA (5 mM final), or eptifibatide (Millennium Pharmaceuticals/Schering, 300 μM final) and saturating concentrations of fluorescent antibodies or isotype controls. Samples were fixed and analyzed on a FACSCalibur flow cytometer using CellQuest software (BD Biosciences). Both forward and side scatter detectors were set on logarithmic scales, and the analysis gate was set on the major population of platelets. The percentage of positive platelets and their mean fluorescent intensity were calculated from single-parameter histograms of a minimum of ten thousand events from the gated region.

Western blot analysis of protein tyrosine phosphorylation

For analysis of integrin β3 phosphorylation in human platelets, PRP was incubated with eptifibatide and/or heparin, washed, then lysed and immunoprecipitated with an anti-β3 monoclonal antibody (mAb) (PM6/13, Millipore). Samples were analyzed by Western blotting (Western Breeze kit, Invitrogen) using a polyclonal rabbit antibody directed against a peptide from human integrin β3 containing phosphotyrosine (pY)759 (Santa Cruz Biotechnology). After detection of phosphorylated β3, the membranes were stripped (ReBlot Plus Strong, Millipore) and total β3 was detected using a mouse mAb (clone 1, BD Transduction Laboratories). Scanned films were analyzed using ImageJ (http://rsb.info.nih.gov/ij/index.html), Microsoft Excel, and Prism5 (GraphPad) software.

KαIIbβ3 cells, derived from K562 cells transfected with plasmids expressing integrins αIIb and β3, were cultured as previously described [20]. To assay integrin β3 phosphorylation, cells were washed and spread on fibrinogen-coated Petri dishes. Nonadherent cells were removed, the adherent cells were lysed directly in sample buffer, and total protein analyzed by Western blotting. For detection of src activation, polyclonal anti-pY416 and monoclonal rabbit anti-src (Cell Signaling Technologies) were used as the primary antibodies.

Preparation, expression, and purification of αIIb and β3proteins and fragments

Intact human αIIbβ3 was purified from platelet concentrates as previously described [15]. Recombinant fragments of αIIb and the extracellular domain of β3 were generated by PCR cloning into His-fusion vectors and expressed in BL21 (DE3) bacteria (αIIb fragments) or S2 insect cells (β3extracellular domain). The αIIb fragments encompassed amino acids 1–269 (Region 1), 263–559 (Region 2), and 547–867 (Region 3) (Supplemental Figs. 1 and 2). The β3 extracellular domain included amino acids 28–716. For purification of αIIb fragments, inclusion bodies were solubilized and purified on a cobalt affinity column following manufacturer's protocols (Talon, Clontech). The β3 extracellular domain was isolated from supernatants of S2 cells by affinity chromatography on Talon resin.

Surface plasmon resonance detection of heparin binding

A gold-coated sensor chip (Nippon Laser and Electronics Lab) was coated with glucosamine N-sulfate (6-O-sulfate)-iduronic acid (2-O-sulfate) (GlcNS6S-IdoA2S) and placed in the sensing channel of a 2-channel SPR instrument (SPR-670, Moritex, Yokohama, Japan) [21,22]. A control chip coated with D-maltose was placed in the reference channel. Proteins in 0.1% TritonX-100 in PBS were injected simultaneously into both channels. Binding was detected, and binding curves and kinetic parameters calculated, using the manufacturer's software.

Analysis of heparin binding sites and αIIbβ3 conformation

Analyses were performed on the crystal structure of αIIbβ3 reported by Zhu, et al (PDB ID: 3FCS) [23] using the program Cn3D (version 4.1; http://www.ncbi.nlm.nih.gov/Structure/CN3D/cn3d.shtml).

Results

Heparin induces conformational changes in platelet integrin αIIbβ3

We have previously shown that integrin αIIbβ3 is the major binding site for heparin on platelets [15]. To determine whether heparin interaction directly modulates integrin αIIbβ3 conformation, we used flow cytometry to measure the binding of a panel of antibodies to activation-dependent epitopes on human platelets. These epitopes are masked in the resting form of αIIbβ3, and are exposed by conformational activation of the receptor and high-affinity ligand binding. The antibodies LIBS-1 and −6 bind to ligand-associated epitopes on integrin β3, while PMI-1 and PAC-1 bind to αIIb [24–26]. PRP from five different normal volunteers was incubated with the respective antibodies in PBS alone, or in the presence of 5 μg/ml heparin. Fig. 1A shows the change in the percentage of platelets positive for each epitope, expressed as the ratio (% with heparin/% without heparin). Heparin increased the binding of all the activation-dependent antibodies, from an average of 1.4- (LIBS-1) to 1.8-fold (PAC-1). The increases in binding of both LIBS-6 and PAC-1 in the presence of heparin were statistically significant ($p < .05$, t-test). The presence of heparin alone did not induce the expression of the activation-dependent marker p-selectin (Fig. 1A), suggesting that heparin binding alone was not sufficient to induce platelet activation.

The effect of heparin on ligand-induced conformational changes was assessed in a second set of experiments. PRP was incubated with the integrin antagonist eptifibatide, and the binding of LIBS-1 and 6 was measured in the presence or absence of heparin. Although eptifibitide prevents αIIbβ3 signaling and platelet aggregation [18], biophysical measurements indicate that eptifibitide binding can induce partial activation of the receptor [27]. Because a large

Please cite this article as: Yagi M, et al, Heparin modulates the conformation and signaling of platelet integrin αIIbβ3, Thromb Res (2011), doi:10.1016/j.thromres.2011.11.054

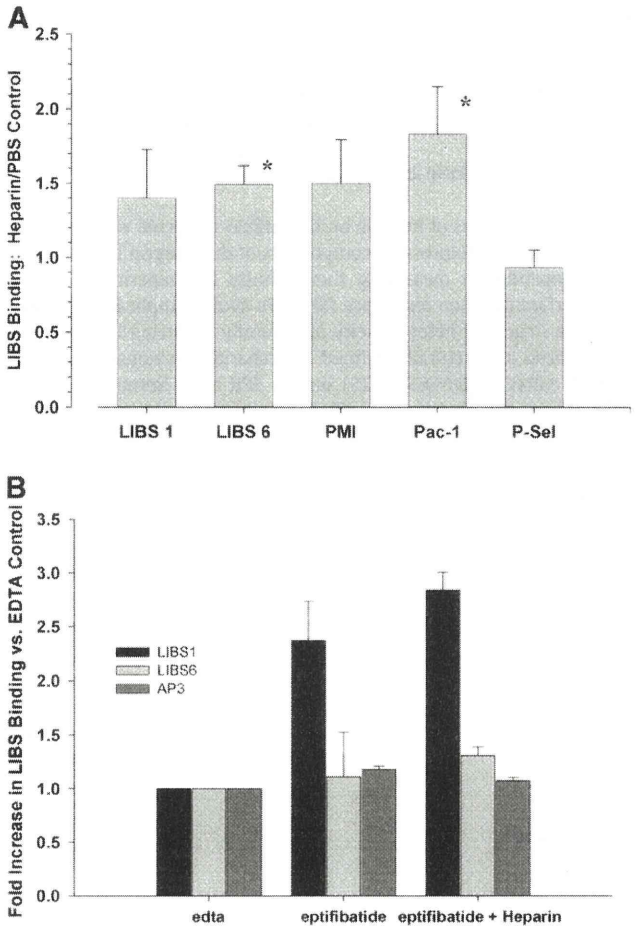

Fig. 1. Conformational changes in αIIbβ3 measured by flow cytometry. A, Relative binding of Pac-1, LIBS, and p-selectin antibodies to platelets in the absence of ligand. PRP was incubated with the indicated antibodies in the presence of 5 μg/ml heparin. Data are expressed as the percentage positive platelets for heparin treatment divided by PBS control (means ± SEM of 5 different subjects). The addition of heparin increased LIBS-1 and PAC-1 binding significantly more than that of p-selectin, which was no different than PBS controls ($p<.05$, *t*-test). B, Increased binding of LIBS1 but not LIBS6 in the presence of heparin and ligand. PRP was incubated with EDTA (5 mM) or eptifibatide (300 μM) with and without heparin (5 μg/ml). Separate aliquots were incubated with the conformation-dependent antibodies LIBS-1, LIBS-6, or AP3(which recognizes all conformations of αIIbβ3). The fold increase in mean fluorescent intensity of antibody binding over EDTA controls is shown. Values are the means ± SEM of 2 studies.

percentage of platelets were LIBS-positive in the presence of epitifibatide, further changes are expressed as the ratio of the mean fluorescence intensity in the presence or absence of heparin. Fig. 1B illustrates that the addition of heparin increases the binding of LIBS-1 in the presence of eptifibitide, while that of LIBS-6 is largely unaffected. Total surface expression of αIIbβ3, as measured by the antibody AP3, showed no changes with the different treatments.

Heparin augments signal transduction through integrin αIIbβ3

Ligand binding to integrin αIIbβ3 triggers signaling that ultimately results in platelet activation [16–18]. Because heparin appears to augment the ligand-bound conformation of αIIbβ3, we assayed the effect of heparin on tyrosine phosphorylation of the β3 cytoplasmic tail, one of the earliest signaling events of outside-in signaling. PRP was incubated with eptifibatide and varying amounts of heparin, and the phosphorylation of tyrosines in the β3 cytoplasmic tail was measured by Western blotting. To account for differences in gel loading, band intensities in the phosphotyrosine blots were normalized with the intensities of the total β3 integrin bands before assessing the effect of heparin addition. Fig. 2A shows that, while neither heparin nor eptifibatide alone stimulate tyrosine phosphorylation of the

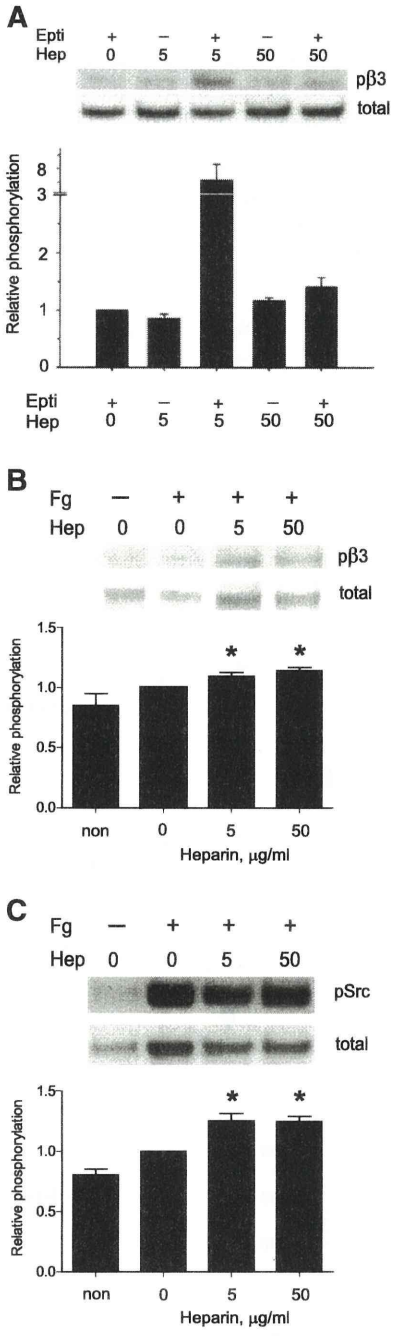

Fig. 2. Phosphorylation of the integrin β3 cytoplasmic tail and src in human platelets and KαIIbβ3 cells. A, Human PRP was incubated with eptifibatide (300μMolar) and/or heparin (5 or 50 μg/ml) and β3 phosphorylation measured as described in the Methods. Values are the means ± SEM of 2 independent experiments, expressed as the fold change in β3 phosphorylation compared to ligand alone. The Western blot of a representative experiment is depicted. B, Washed KαIIbβ3 cells were adhered to immobilized fibrinogen in the absence or presence of heparin (means ± SEM of 3 studies). Asterisks indicate $p<0.05$ (*t*-test) compared to the PBS control. C, Phosphorylation of src at tyr418 in KαIIbβ3 cells adhering to fibrinogen with or without heparin. Values are the means ± SEM of five experiments. Asterisks indicate $p<0.05$ (*t*-test) compared to control.

Please cite this article as: Yagi M, et al, Heparin modulates the conformation and signaling of platelet integrin αIIbβ3, Thromb Res (2011), doi:10.1016/j.thromres.2011.11.054

β3 cytoplasmic domain, a low concentration of heparin (5 μg/ml) significantly increased phosphorylation in response to eptifibatide.

To confirm that this effect was integrin-dependent, we repeated the experiment using K562 cells transfected with αIIbβ3 (KαIIbβ3) [20,28]. These cells have been shown to bind fibrinogen, and this model has been useful in dissecting integrin signaling. By flow cytometry, KαIIbβ3 cells do not express significant levels of other integrins (not shown). Fig. 2B illustrates that phosphorylation of integrin β3 in KαIIbβ3 cells adhering to immobilized fibrinogen is significantly increased in the presence of heparin. As in platelets, this effect is observed at low concentrations of heparin, and is not increased at higher concentrations.

Another early marker of outside-in signaling by integrin αIIbβ3 is activation of the tyrosine kinase src, which is constitutively associated with the β3 cytoplasmic tail [29]. In response to ligand binding, src is dephosphorylated at tyrosine-529 and phosphorylated at tyrosine-418, activating the kinase and initiating platelet activation. Fig. 2C shows that, in KαIIbβ3 cells adhering to fibrinogen, heparin significantly increases phosphorylation of endogenous src at tyrosine-418. These results indicate that heparin binding can amplify ligand-induced signaling through integrin αIIbβ3.

Identification of heparin-binding regions of αIIbβ3

The binding sites of heparin on the αIIbβ3 molecule were mapped more precisely by expressing components of the integrin heterodimer, and independently measuring their affinity for heparin structures, using surface plasmon resonance (SPR). To avoid complications arising from the structural heterogeneity of naturally occurring heparins, we immobilized a structurally defined disaccharide previously shown to bind to αIIbβ3 (GlcNS6S-Ido2S) on the SPR chip. Immobilization of the purified disaccharide also effectively increases the concentration

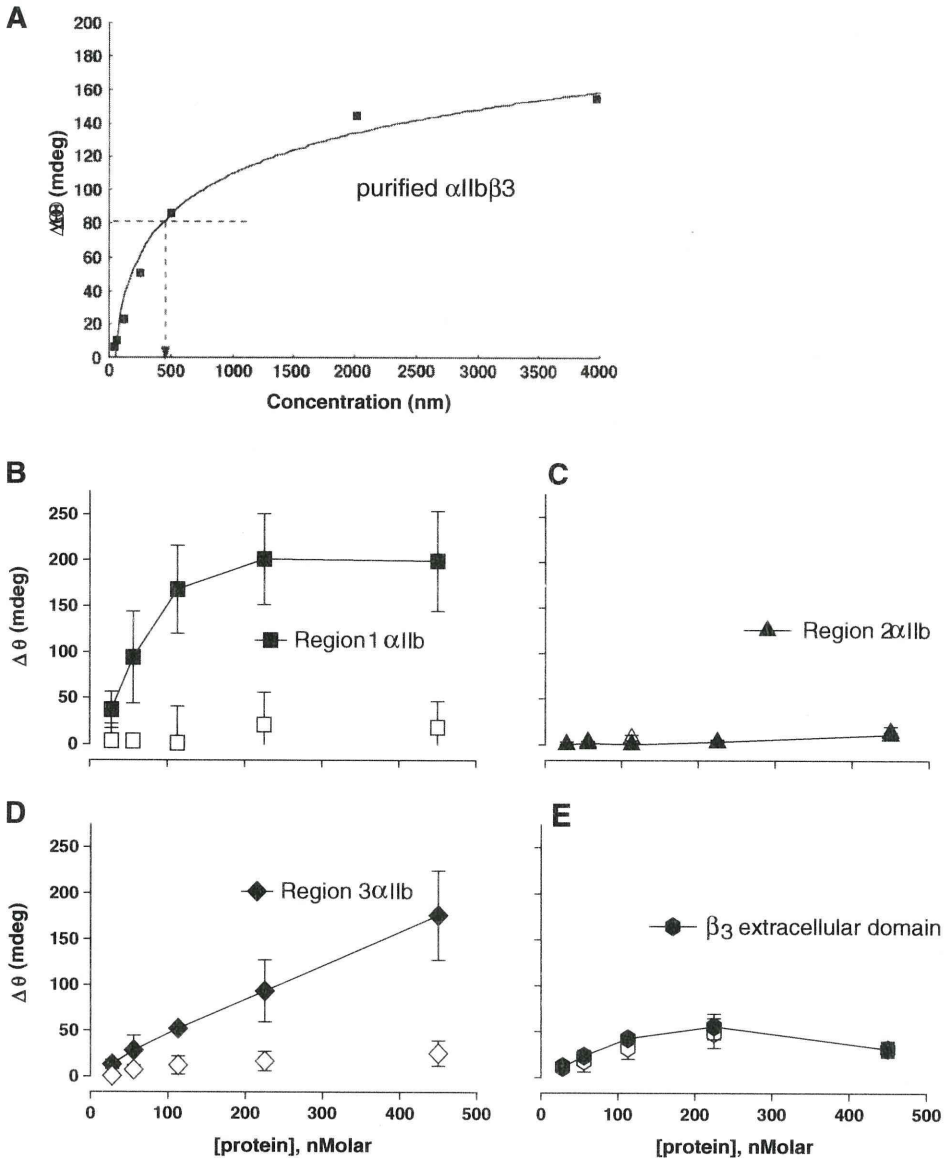

Fig. 3. SPR binding analyses. A, αIIbβ3. A typical binding experiment is illustrated, in which a range of concentrations of purified human αIIbβ3 were perfused over the sugar chip immobilized with a structurally defined synthetic oligosaccharide of GcNS6S-Ido2S known to bind to the platelet. B-E, recombinant fragments of αIIb and β3. For each fragment, binding to the defined heparin oligosaccharide is illustrated by the filled symbols, and binding to the control maltose chip by the open symbols. Values are the means ± SD from three independent experiments.

Please cite this article as: Yagi M, et al, Heparin modulates the conformation and signaling of platelet integrin αIIbβ3, Thromb Res (2011), doi:10.1016/j.thromres.2011.11.054

of the active structure [22]. Binding was first measured to intact integrin αIIbβ3 purified from human platelets, and then to isolated fragments of αIIb and β3 individually. Increasing concentrations of protein in buffer were passed over the immobilized oligosaccharide to assess binding. Fig. 3A illustrates the binding curve for purified platelet-derived αIIbβ3, where the K_D was calculated to be 440nM. Fig. 3 (B-E) are the binding curves for individual fragments of αIIb and the extracellular domain of β3, and Table 1 summarizes the dissociation constants derived from these experiments. Region 1 of αIIb (corresponding to the amino-terminal half of the head domain [30]) and Region 3 (containing part of the thigh and both calf domains) showed significant binding to the immobilized disaccharide. In contrast, the extracellular domain of β3 and αIIb Region 2 (the carboxy-terminal half of the head and adjoining thigh domain) did not appear to bind. These assays were repeated using unfractionated heparin immobilized on the SPR chip, which confirmed that only Regions 1 and 3 from αIIb bound to heparin (not shown), with affinities similar to the disaccharide. The calculated K_D for Region 1 was 68.1nM for the disaccharide (Table 1) and 106.6nM for unfractionated heparin.

Discussion

We have previously shown that heparin binds to platelet integrin αIIbβ3, resulting in platelet activation and aggregation [12,15]; however, in those experiments it was unclear if heparin binding alone could activate signaling. These experiments were undertaken to address this question. The flow cytometry experiments indicate that heparin binding can induce conformational changes in αIIbβ3 similar to those resulting from ligand binding, and that heparin augments the conformational changes induced by ligand binding. The absence of increased p-selectin expression in response to heparin alone suggests that platelets are not fully activated by heparin binding. Analyses of β3 tyrosine phosphorylation and src activation further confirm that heparin alone does not produce detectable outside-in signaling, but in the presence of ligand, heparin significantly enhances signaling through αIIbβ3, both in platelets and in transfected cells expressing the integrin. Finally, through analysis of heparin-binding to isolated fragments of αIIbβ3, we mapped putative heparin-binding sites to the headpiece and genu of αIIb.

Gao et al. have also recently reported that heparin potentiates signaling through platelet αIIbβ3 [19]. Their study demonstrated that heparin augments phosphorylation of FAK and Akt in response to ligand binding. This current report extends these findings by documenting that the earliest events of the outside-in signaling cascade are potentiated by heparin. By using the K562 model system, which is devoid of other platelet receptors, we were able to show that heparin binding increases phosphorylation of the integrin β3 cytoplasmic domain and activation of the associated src kinase in response to ligand binding. Taken together, these results indicate that heparin binding results in platelet stimulation at least in part by the induction or stabilization of an activated conformation of αIIbβ3, thus facilitating ligand binding to the integrin, and amplifying outside-in signaling and platelet activation.

Mapping the binding sites of heparin on the αIIbβ3 molecule suggests a model for this mechanism. Classical linear heparin-binding motifs composed of appropriately spaced cationic residues [31–33] can be found in the extracellular domain of β3 and Region 2 of αIIb. However, the results of the binding studies demonstrated that neither β3 nor Region 2 bound heparin, while Regions 1 and 3 of αIIb bound with significant affinity to heparin and its disaccharide. Additionally, the overall densities of arginine and lysine residues in Regions 1–3 do not correlate with their heparin-binding affinity (6.3% arginine/lysine residues in Region 1, 8.8% in Region 2, 5.7% in Region 3). Thus, it seems unlikely that heparin is binding to linear or random distributions of basic amino acids in the recombinant fragments, suggesting that the major heparin binding site(s) are formed by folding of the αIIb polypeptide. One caveat is that these recombinant proteins may not be folded in precisely the same conformation as the native protein.

Table 1
Dissociation Constants for purified αIIbβ3 and Recombinant Portions of αIIbβ3.

	K_D (nMolar)
native αIIbβ3	440
Region 1 αIIb	68.1
Region 2 αIIb	no binding
Region 3 αIIb	169
recombinant β3	no binding

The crystal structure of the αIIbβ3 extracellular domain [23] reveals that several clusters of arginine and lysine residues are located on the external face of the protein. Region 1 (which binds heparin) contains a large cluster on one face of the β-propeller (Fig. 4A and B). In particular, the arginines at positions 73, 77, 139, 140, and 208, along with lysine 118, are located around the cap subdomain of αIIb, adjacent to the residues essential for fibrinogen binding [34]. The basic amino acids contained in Region 3 (which also binds heparin) also appear to fall in several clusters (Fig. 4C and D). Two clusters are located on either side of the genu, in the thigh and calf-1 domains, and a third on the opposite face of calf-1.

This correlation between experimental binding studies and the crystallographic model of αIIb offers new hypotheses about how heparin modulates integrin function. Heparin may interact with the cap subdomain, thereby modifying the conformation of the ligand-binding site. In addition, binding of a charged polysaccharide chain to the clustered basic amino acids on either side of the genu could facilitate or stabilize the opening of the thigh and calf domains, extending the leg and exposing the ligand-binding site. Finally, the third cluster of basic amino acids on calf-1 appears to lie near binding sites for calcium in the β-propeller in the inactive conformation, so binding of heparin to this cluster could potentially modify interactions of αIIb with divalent cations [34]. Others have shown that opening of the leg alone can increase the affinity of αIIbβ3 for ligand. Mutation of residues surrounding the genu that constrain the opening of the leg inhibits activation-induced increases in binding affinity [35,36]. In contrast, introduction of a glycosylation site "behind" the genu, which prevents the leg from closing, results in constitutive high-affinity ligand binding [36]. Similarly, mutations of β3 that destabilize interactions with the αIIb leg, therefore favoring a more extended resting conformation, also confer constitutive high-affinity ligand binding [37]. Thus, heparin, by binding to one or more sites on the αIIb polypeptide, may stabilize an open, partially activated, conformation of αIIbβ3.

The demonstration that heparin can modulate the behavior of integrin αIIbβ3 may have implications beyond the regulation of platelet activation [14]. As an antithrombotic drug, unfractionated heparin may have theoretical drawbacks, particularly when administered to patients with systemic platelet activation, or in combination with integrin antagonists like eptifibatide that may synergistically stabilize activated conformations of αIIbβ3. Heparin has also been shown to affect processes such as tumor metastasis and leukocyte extravasation [38], in which the interactions of various integrins with their ligands appear to play a role in regulating cell adhesion. Thus, further understanding of the role of heparin in modulation of cell adhesion may advance the use of oligosaccharides derived from heparin for therapeutic purposes in cancer and inflammatory disorders, as well as in regulating coagulation.

Conflict of interest

No potential conflict of interest exists for any of the study authors.

Please cite this article as: Yagi M, et al, Heparin modulates the conformation and signaling of platelet integrin αIIbβ3, Thromb Res (2011), doi:10.1016/j.thromres.2011.11.054

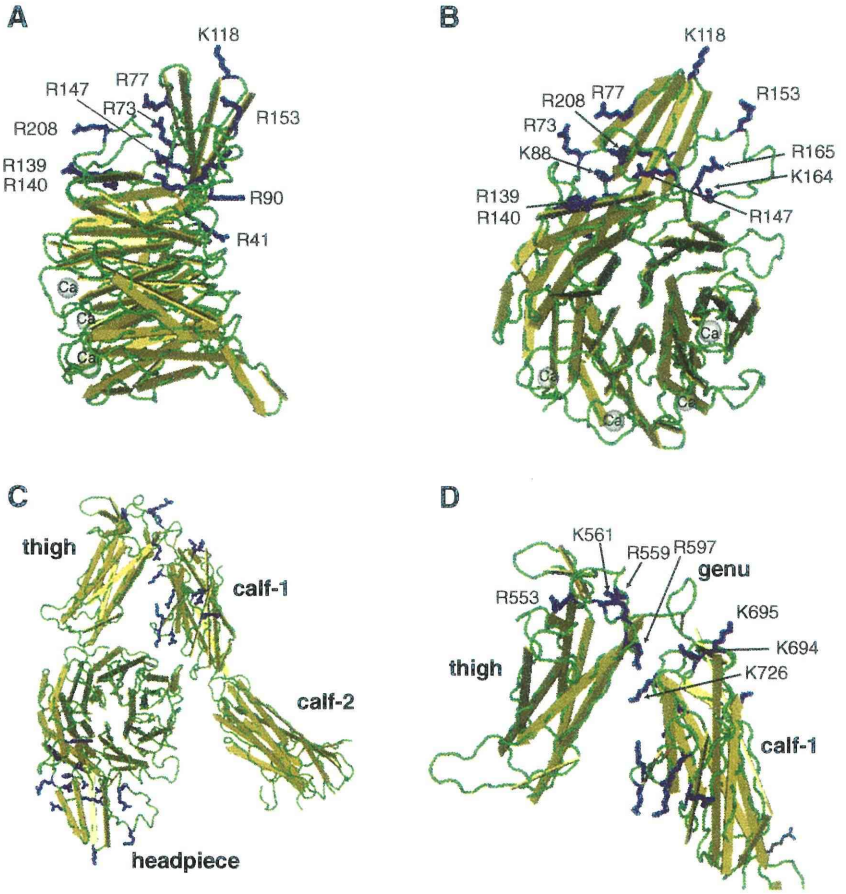

Fig. 4. Clustering of basic amino acids in αIIb. Locations of basic amino acids in αIIb, based on the crystal structure of Zhu, et al [26]. Figures were generated using Cn3D (version 4.1, http://www.ncbi.nlm.nih.gov/Structure/CN3D/cn3d.shtml). A & B, two views of the αIIb headpiece. B is rotated approximately 90° from A. The αIIb protein backbone is in green. The side chains of the Arg (R) and Lys (K) residues located in Region 1 (AA 1–262) are represented by blue sticks. C, an overview of the closed form of the αIIb chain. The Arg and Lys side chains in Regions 1 and 3 are depicted as blue sticks. **D**, the thigh and calf-1 domains of αIIb. The Arg and Lys residues within 15 Å of the genu are identified.

Acknowledgements

This work was supported by grants from the National Institutes of Health (HL39903) and the Department of Veterans Affairs to MS.

Appendix A. Supplementary data

Supplementary data to this article can be found online at doi:10.1016/j.thromres.2011.11.054.

References

[1] Kelton JG, Warkentin TE. Heparin-induced thrombocytopenia: a historical perspective. Blood 2008;112:2607–16.
[2] Heinrich D, Gorg T, Schulz M. Effects of unfractionated and fractionated heparin on platelet function. Haemostasis 1988;18(Suppl. 3):48–54.
[3] Ellison N, Edmunds Jr LH, Colman RW. Platelet aggregation following heparin and protamine administration. Anesthesiology 1978;48:65–8.
[4] Salzman EW, Rosenberg RD, Smith MH, Lindon JN. Effect of heparin and heparin fractions on platelet aggregation. J Clin Invest 1980;65:64–73.
[5] Thomson C, Forbes CD, Prentice CR. The potentiation of platelet aggregation and adhesion by heparin in vitro and in vivo. Clin Sci Mol Med 1973;45:485–94.
[6] Anand SX, Kim MC, Kamran M, Sharma SK, Kini AS, Fareed J, et al. Comparison of platelet function and morphology in patients undergoing percutaneous coronary intervention receiving bivalirudin versus unfractionated heparin versus clopidogrel pretreatment and bivalirudin. Am J Cardiol 2007;100:417–24.
[7] Furman MI, Kereiakes DJ, Krueger LA, Mueller MN, Pieper K, Broderick TM, et al. Leukocyte-platelet aggregation, platelet surface p-selectin and platelet surface glycoprotein IIIa after percutaneous coronary intervention: effects of dalteparin or unfractionated heparin in combination with abciximab. Am Heart J 2001;142:790–8.
[8] Cella G, Scattolo N, Luzzatto G, Girolami A. Effects of low-molecular-weight heparin on platelets as compared with commercial heparin. Res Exp Med (Berl) 1984;184:227–9.
[9] Mikhailidis DP, Fonseca VA, Barradas MA, Jeremy JY, Dandona P. Platelet activation following intravenous injection of a conventional heparin: absence of effect with a low molecular weight heparinoid (Org 10172). Br J Clin Pharmacol 1987;24:415–24.
[10] Westwick J, Scully MF, Poll C, Kakkar VV. Comparison of the effects of low molecular weight heparin and unfractionated heparin on activation of human platelets in vitro. Thromb Res 1986;42:435–47.
[11] Sobel M, Adelman B. Characterization of platelet binding of heparins and other glycosaminoglycans. Thromb Res 1988;50:815–26.
[12] Suda Y, Marques D, Kermode JC, Kusumoto S, Sobel M. Structural characterization of heparin's binding domain for human platelets. Thromb Res 1993;69:501–8.
[13] Suda Y, Bird K, Shiyama T, Koshida S, Marques D, Fukase K, et al. Synthesis and biological activity of a model disaccharide containing a key unit in heparin for binding to platelets. Tetra Lett 1996;37:1053–6.
[14] Da Silva MS, Horton JA, Wijelath JM, Blystone LW, Fish WR, Wijelath E, et al. Heparin modulates integrin-mediated cellular adhesion: specificity of interactions with α and β integrin subunits. Cell Commun Adhes 2003;10:59–67.
[15] Sobel M, Fish W, Toma N, Luo S, Bird K, Blystone SD, et al. Heparin modulates integrin function in human platelets. J Vasc Surg 2001;33:587–94.
[16] Bennett JS, Berger BW, Billings PC. The structure and functions of platelet integrins. J Thromb Haemost 2009;7(Suppl 1):200–5.
[17] Li Z, Delaney K, O'Brien K, Du X. Signaling during platelet adhesion and activation. Arterioscler Thromb Vasc Biol 2010;30:2341–9.
[18] Phillips DR, Nannizzi-Alaimo L, Prasad KS. β3 tyrosine phosphorylation in αIIbβ3 (platelet membrane GP IIb-IIIa) outside-in integrin signaling. Thromb Haemost 2001;86:246–58.
[19] Gao C, Boylan B, Fang J, Wilcox DA, Newman DK, Newman PJ. Heparin promotes platelet responsiveness by potentiating αIIbβ3-mediated outside-in signaling. Blood 2011;117:4946–52.

Please cite this article as: Yagi M, et al, Heparin modulates the conformation and signaling of platelet integrin αIIbβ3, Thromb Res (2011), doi:10.1016/j.thromres.2011.11.054

[20] Blystone SD. Kinetic regulation of β3 integrin tyrosine phosphorylation. J Biol Chem 2002;277:46886–90.
[21] Koshida S, Suda Y, Fukui Y, Sobel M, Kusumoto S. Model compounds containing key platelet-binding disaccharide units in heparin: synthesis and binding activity to platelets. Proc Chem Soc Japan 1999;75:688.
[22] Koshida S, Suda Y, Sobel M, Kusumoto S. Synthesis of oligomeric assemblies of a platelet-binding key disaccharide in heparin and their biological activities. Tetra Let 2001;42:1289–92.
[23] Zhu J, Luo B-H, Xiao T, Zhang C, Nishida N, Springer TA. Structure of a complete integrin ectodomain in a physiologic resting state and activation and deactivation by applied forces. Mol Cell 2008;32:849–61.
[24] Shattil SJ, Hoxie JA, Cunningham M, Brass LF. Changes in the platelet membrane glycoprotein IIb.IIIa complex during platelet activation. J Biol Chem 1985;260:11107–14.
[25] Ginsberg M, Lightsey A, Kunicki TJ, Kaufman A, Marguerie G, Plow E. Divalent cation regulation of the surface orientation of platelet membrane glycoprotein IIb: correlation with fibrinogen binding function and definition of a novel variant of Glanzmann's thrombasthenia. J Clin Invest 1986;78:1103–11.
[26] Frelinger AL, Du X, Plow EF, Ginsberg M. Monoclonal antibodies to ligand-occupied confomers of integrin αIIbβ3 (glycoprotein IIb-IIIa) alter receptor affinity, specificity, and function. J Biol Chem 1991;266:17106–11.
[27] Hantgan RR, Stahle MC, Connor JH, Connor RF, Mousa SA. αIIbβ3 priming and clustering by orally active and intravenous integrin antagonists. J Thromb Haemost 2006;5:542–50.
[28] Blystone SD, Lindberg FP, LaFlamme SE, Brown EJ. Integrin β3 cytoplasmic tail is necessary and sufficient for regulation of α5β1 phagocytosis by αvβ3 and integrin-associated protein. J Cell Biol 1995;130:745–54.
[29] Shattil SJ. Integrins and src:dynamic duo of adhesion signaling. Trends Cell Biol 2005;15:399–403.
[30] Arnaout MA, Mahalingham B, Xiong JP. Integrin structure, allostery, and bidirectional signaling. Ann Rev Cell Dev Biol 2005;21:381–410.
[31] Cardin AD, Weintraub HJ. Molecular modeling of protein-glycosaminoglycan interactions. Arteriosclerosis 1989;9:21–32.
[32] Rastegar-Lari G, Villoutreix BO, Ribba AS, Legendre P, Meyer D, Baruch D. Two clusters of charged residues located in the electropositive face of the von Willebrand factor A1 domain are essential for heparin binding. Biochemistry 2002;41:6668–78.
[33] Sobel M, Soler DF, Kermode JC, Harris RB. Localization and characterization of a heparin binding domain peptide of human von Willebrand factor. J Biol Chem 1992;267:8857–62.
[34] Kamata T, Tien KK, Irie A, Springer TA, Takada Y. Amino acid residues in the αIIb subunit that are critical for ligand binding to integrin αIIbβ3 are clustered in the β propeller model. J Biol Chem 2001;276:44275–83.
[35] Blue R, Li J, Steinberger J, Murcia M, Filizola M, Coller BS. Effects of limiting extension at the αIIb genu on ligand binding to αIIbβ3. J Biol Chem 2010;285:17604–13.
[36] Kamata T, Handa M, Ito S, Sato Y, Ohtani T, Kawai Y, et al. Structural requirements for activation in αIIbβ3 integrin. J Biol Chem 2010;285:38428–37.
[37] Donald JE, Zhu H, Litvinov RI, DeGrado WF, Bennett JS. Identification of interacting hot spots in the β3 integrin stalk using comprehensive interface design. J Biol Chem 2010;285:38658–65.
[38] Borsig L. Antimetastatic activities of heparins and modified heparins. Experimental evidence. Thromb Res 2010;125(Suppl 2):S66–71.

Please cite this article as: Yagi M, et al, Heparin modulates the conformation and signaling of platelet integrin αIIbβ3, Thromb Res (2011), doi:10.1016/j.thromres.2011.11.054